SCIENTIFIC REPORTS

OPEN

SUBJECT AREAS:
HIGH-THROUGHPUT SCREENING
COMPUTATIONAL MODELS

Received
3 October 2013

Accepted
19 December 2013

Published
20 January 2014

Correspondence and requests for materials should be addressed to L.M. (lmarinelli@unina.it) or M.S. (mariano.stornaiuolo@gmail.com)

Beyond radio-displacement techniques for Identification of CB_1 Ligands: The First Application of a Fluorescence-quenching Assay

Agostino Bruno, Francesca Lembo, Ettore Novellino, Mariano Stornaiuolo & Luciana Marinelli

Department of Pharmacy, University of Naples ''Federico II'', via D. Montesano 49, 80131 Naples, Italy.

Cannabinoid type 1 Receptor (CB_1) belongs to the GPCR family and it has been targeted, so far, for the discovery of drugs aimed at the treatment of neuropathic pain, nausea, vomit, and food intake disorders. Here, we present the development of the first fluorescent assay enabling the measurement of kinetic binding constants for CB_1orthosteric ligands. The assay is based on the use of T1117, a fluorescent analogue of AM251. We prove that T1117 binds endogenous and recombinant CB_1 receptors with nanomolar affinity. Moreover, T1117 binding to CB_1 is sensitive to the allosteric ligand ORG27569 and thus it is applicable to the discovery of new allosteric drugs. The herein presented assay constitutes a sustainable valid alternative to the expensive and environmental impacting radiodisplacement techniques and paves the way for an easy, fast and cheap high-throughput drug screening toward CB_1 for identification of new orthosteric and allosteric modulators.

Cannabinoid (CB) receptors are human receptors responsible for the prominent effects (hypokinesia, catalepsy, analgesia and stimulation of food intake) of (−)-Δ^9-tetrahydrocannabinol (Δ^9-THC), the main psychotropic constituent of cannabis[1–3]. At least three CB receptors are expressed in human tissues: (*i*) CB_1 receptors, which are found predominantly at central and peripheral nerve terminals, where they mediate inhibition of transmitter release[2,4], (*ii*) CB_2 receptors, which are mainly located on immune cells, where they modulate cytokines release[2,5], and (*iii*) GPR55 receptors, which have been recently proven to bind cannabinoids and to be localized in adrenals, in the gastrointestinal tract as well in the central nervous system, even if at much lower level than CB_1[6]. Both CB_1 and CB_2 receptors are coupled to $G_{i/o}$ proteins, negatively to Adenylate Cyclase and positively to mitogen-activated protein kinase[7,8].

Endogenous agonists of CB receptors like arachydonoylethanolamide (anandamide) and 2-arachidonoyl glycerol have been identified[9,10], as well as several CB_1 and CB_2 selective agonists and antagonists have been synthetically developed[2]. Some of them behave as inverse agonists, an indication that CB_1 and CB_2 receptors can exist in a constitutive active state[11]. At least three orthosteric ligands of CB receptors (Cesamet[12], Marinol[13], and Sativex[14]) are already in clinic, with them being prescribed to reduce chemotherapy-induced nausea, stimulate appetite, reduce neuropathic pain and as adjunctive analgesic treatment for patients with advanced cancer[2]. On contrary, Rimonabant, an inverse agonist of CB receptors, was firstly commercialized as anorectic antiobesity drug, and then suspended due to the psychiatric problems described in treated patients[15]. The withdrawal of Rimonabant once more highlights the need of fine-tuning CB_1 functionality for development of a safe drug. In that regard allosteric ligands offer great opportunities and great strides have been performed in the CB_1 field[16–18] for their discovery.

Indeed, the existence of an allosteric site on the CB_1 receptors was experimentally demonstrated[19] and the finding and characterization of CB_1 allosteric modulators is still object of intense research[16,17]. Among CB_1 allosteric ligands, ORG27569 was proven to modulate the rate of binding[20–22] for agonists and inverse agonists without affecting their binding constants[23,24].

Nowadays, affinities and binding parameters of ligands for the orthosteric and allosteric binding site of the CB receptors are usually measured using radioligand displacement assays. Besides the considerable costs of those assay, the lipophilicity and the low degree of solubility in water of the majority of CB ligands complicate the above-mentioned procedure[25–27].Indeed, the compounds either stick non-specifically to membranes or to the

filters used to separate their unbound pool from the receptor-bound one. This, in turn, alters the correct measurement of the concentration of free ligand and thus the values of binding and kinetic parameters[25].

Recently, a fluorescent tetra-methyl-rhodamine (TAMRA) labeled form of the CB receptor inverse agonist AM251, namely T1117 (Fig. 1), was commercialized, thus paving the way for the development of a new fluorescence assay in the CB receptor field. However, the use of fluorescently labeled ligands for binding studies needs preliminary proofs. The reduction in affinity for the target, common in fluorescently modified ligands, does not have to compromise precision, accuracy and usefulness of the assay[28,29]. As regards T1117, radio-displacement assays have reported decreased affinity for CB receptors compared to AM251[30], while an increased specificity for GPR55 was reported although few details have been shown[30,31].

In line with the published results, we observe a moderate decrease of affinity for both the endogenously and eterologously expressed CB_1 receptor (IC50 = 8 nM vs 450 nM, for AM251[32] and T1117, respectively). Herein, computational approaches were used to give insight about possible reasons behind the lower affinity of T1117. Upon binding to CB_1 receptor, T1117 gets fluorescently quenched allowing the monitoring of the binding event. This prompted us to develop and set up a fast and easy fluorescent-based assay amenable for high throughput screening of orthosteric as well as allosteric CB ligands. The designed assay not solely allows the measurement of affinity constants, such as pK_i and B_{max}, of new drugs, but allows also detection of the k_{off} and k_{on}, thus giving precious insights on the kinetic aspect of the binding process. The newly developed method turned out to be extremely useful also in the study of allosteric ligands. As proof of concept, the ORG27569 binding towards CB_1 was assessed and perfectly reproduced the reported reduction in the B_{max} of inverse agonist for CB_1. Amenability for high-throughput screening and automatation on one hand, the environmental sustainability and the cost of a T1117 based assay, on the other, locate it among the most valid experimental platform for identification of new CB_1 ligands.

Results

Fluorescence behavior of T1117 upon binding to CB_1 receptor. We started performing equilibrium binding experiments to set up the optimal assay condition. Rat Brain Membranes were incubated with 500 nM T1117 in PBS (Fig. 1) (the solubility of the probe in buffer was poor with the highest solubility reachable in PBS being 5 μM). After 30 minutes of incubation at RT, the fluorescence intensity of T1117 was measured (excitation and emission maxima of T1117 are around 530 and 590 nm, respectively). As shown in Figure 2a and in Supplementary Figure S1, in the presence of membranes the T1117 fluorescence signal decreases compared to the fluorescence of the same amount of probe dissolved in PBS. To monitor change in fluorescence unrelated to the binding to CB_1, membranes were pretreated for 30 minutes with the CB_1 inverse agonist AM251 (5 μM (Fig. 1)) prior incubation with T1117. Upon incubation with AM251, the fluorescence signal of the probe in the membranes is higher than in the absence of the inverse agonist (Fig. 2a). The effect of AM251 is opposite in the absence of membranes. When PBS is supplemented with 5 μM AM251 the fluorescence intensity of T1117 decreases, probably due to absorption of the inverse agonist at the excitation wavelength of the probe (Fig. 2a). The behavior of T1117 in the presence of membranes was somewhat surprising, since the quantum yield of TAMRA is dependent upon polarity of the environment, with the highest yield manifesting in low polarity environments. For this reason, we were expecting an increase in fluorescence intensity after an event of binding. Moreover, fluorescence intensity of T1117 in the presence of membranes and AM251 reaches a much higher value than the one in buffer suggesting a more complex scenario explaining the change in emission property of T1117 in our assay.

Thus, we envisaged the existence of two events happening during our fluorescent binding assay. The first would correspond to the binding of T1117 to CB_1, with the probe being fluorescently-quenched when bound to the receptor. This is not uncommon as it was already seen for other fluorescent probes binding to human receptors[33]. The second event would happen upon displacement of T1117 from CB_1 by AM251. In our hypothesis the probe would remain into membranes due to its hydrophobicity that would discourage it in going back to solution. The apolar lipidic environment of the membranes would be the reason of the increase in T1117 fluorescence emission we register upon displacement by AM251.

With the purpose of verifying our hypothesis, we start demonstrating the tendency of T1117 to remain in membranes upon displacement by AM251. Increasing amount of T1117 were incubated with rat brain membranes or with buffer. After 30 minutes AM251 was added or not to the samples. The mixtures were centrifuged to sediment the membranes and the amount of probe bound to them was measured by absorbance at 530 nm. As shown in Supplementary Figure S2, in the pellet of the samples without membranes we could not detect any trace of T1117 confirming that in our

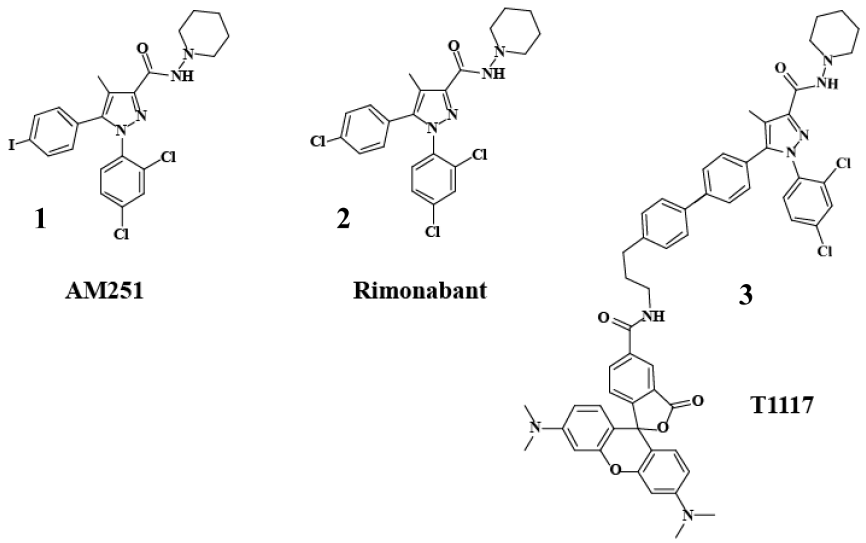

Figure 1 | Structure of AM251, Rimonabant and T1117.

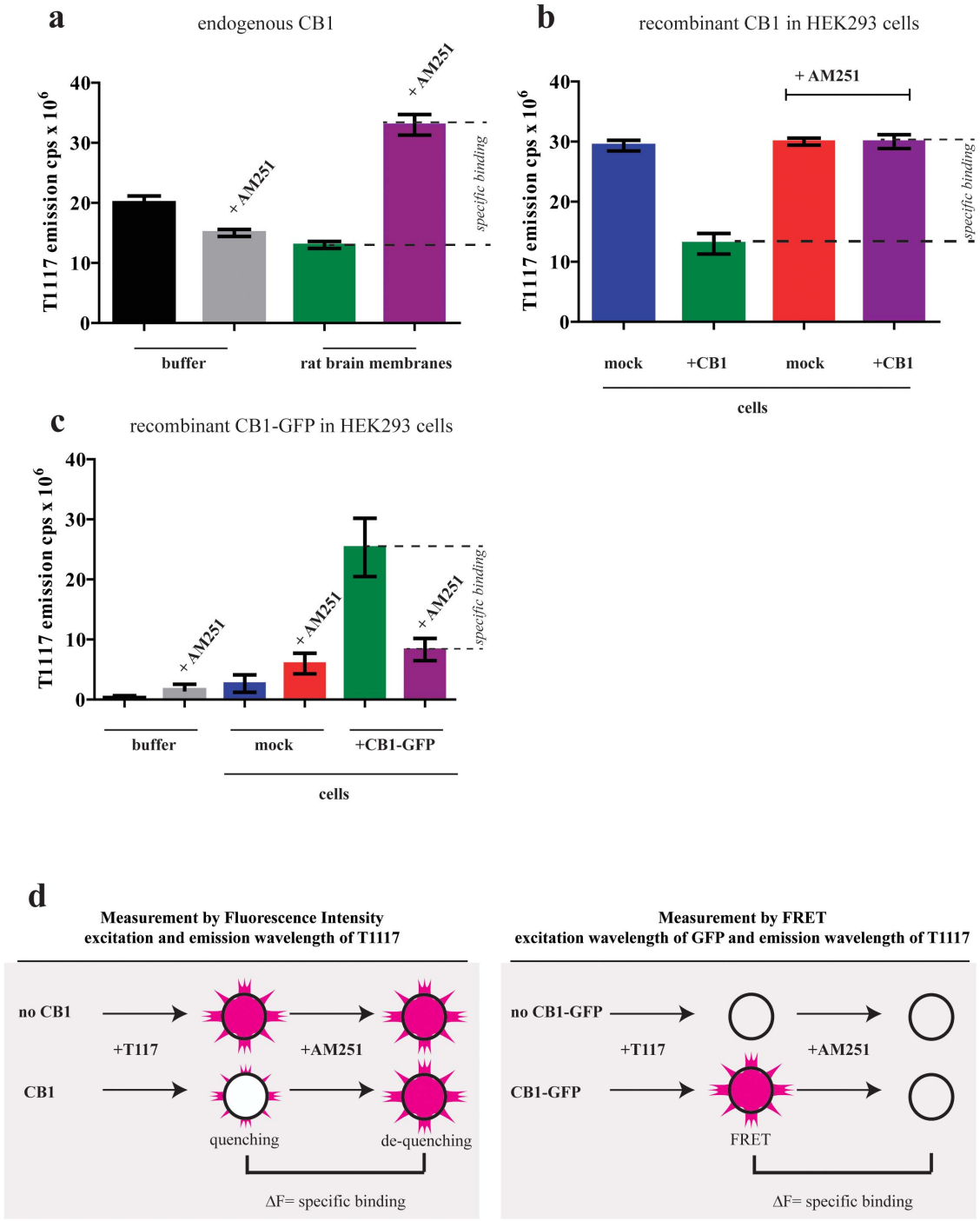

Figure 2 | Fluorescence behavior of T1117 in membranes. (a) Rat brain membranes (30 μg of total protein) were incubated for 30 minutes at RT with T1117 (500 nM) in the presence (purple bar) or in the absence (green bar) of AM251 (5 μM). Samples were excited at 535 nm and fluorescence intensity at 610 nm was recorded and compared with the one of an equal amount of T1117 dissolved in buffer supplemented (gray bar) or not (black bar) with AM251 (5 μM). (b) Human CB_1 receptor was transiently expressed in HEK293 cells. Membranes obtained from mock (red and blue bars) or transfected cells (green and purple bars) were incubated for 30 minutes at RT with T1117 in the presence or in the absence of AM251. Fluorescence intensity at 610 nm was recorded and represented as in a (mean of at least three experiments, s.d. is indicated)). (c) Rat CB_1 –GFP receptor was transiently expressed in HEK293 cells. Membranes obtained from mock (red and blue bars) or transfected cells (green and purple bars) were incubated for 30 minutes at RT with T1117 in the presence or in the absence of AM251. Samples were excited at the excitation wavelength of GFP (485 nm) and fluorescence intensity at 610 nm was recorded and represented as in a (mean of at least three experiments, s.d. is indicated). (d) Schematic drawing of the two protocols described in the text for using T1117 for binding measurement to CB_1 and of the way to measure specific binding. Circles represent cells while the violet star shows the fluorescence intensity of T1117. The text beside them indicates if the cell express or not CB_1. In the left panel is described the measurement of zbinding by Fluorescent Intensity (suitable for binding measurement to endogenously expressed or recombinant non fluorescently-tagged CB_1). Specific binding relates to the difference of T1117 fluorescence before and after displacement. In the right panel is described the measurement of binding by FRET (to use for fluorescently-tagged CB_1 chimeras). Specific binding relates directly to the amount of FRET dependent T1117 fluorescence.

assay condition the probe is soluble. On contrary, in the presence of membranes, T1117 was recovered in the pellet demonstrating its tendency to associate with membranes. Moreover the adding of AM251 did not push the probe back to solution confirming what we register in the fluorescence measurement and thus that, independently from the displacer, T1117 remains bound to membranes. Interesting the association curves of T1117 to membranes are not linear but they reach a plateau after the concentration of 1 μM, moreover the absorbance of T1117 upon displacement by AM251 is increased reflecting the same phenomenon we measure reading the fluorescence of the probe (Fig. 2a).

To further prove our model, the binding of T1117 to CB_1 receptor was followed in an eterologous system where CB_1 was transiently expressed in HEK293 cells. Membranes obtained from mock or CB_1 transfected cells were incubated with 500 nM T1117 in the presence or in the absence of AM251. Upon incubation with T1117, the fluorescence quenching of the probe is visible in membranes obtained from CB_1 expressing cells but not in membranes obtained from untrasfected cells (Fig. 2b) confirming that the fluorescence of T1117 depends on CB_1 binding. Moreover, AM251 is able to determine de-quenching of T1117 only in membranes expressing CB_1 (Fig. 2b).

We confirm these results performing a FACS experiment. A C-terminally tagged version of CB_1 (CB_1-GFP) was transiently expressed in HEK293. After harvesting of the cells, these were treated with 500 nM T1117 followed or not by AM251. CB_1-GFP positive cells were sorted from the untrasfected ones and T1117 fluorescence emission was measured in both the pool of cells (Supplementary Figure S3). Independently by the presence of CB_1-GFP, cells were labeled by T1117. On contrary only in the pool of cell expressing CB_1-GFP a change in fluorescence intensity of T1117 could be registered upon AM251 treatment. These results show the tendency of the probe to associate and to remain attached to cells upon displacement from CB_1. This in turn increases the fluorescence emission of T1117 as it is influenced by the low polarity of the environment and by the absence of quenching water molecules.

To avoid the influence that the change in polarity has on T1117 we changed the setting of our assay measuring binding of the probe to CB_1 by Fluorescence Resonance Energy Transfer (FRET). CB_1-GFP expressing cells were incubated with T1117. Samples were excited at the excitation wavelength of GFP while emission was measured at the one of T1117. FRET is only possible when the two fluorescent moieties are in close proximity (from 10–100 Å). As shown in Figure 2 panel c, FRET from GFP to T1117 can be measured only in cells expressing CB_1-GFP and the energy transfer is reduced by the presence of AM251. The change in polarity of TAMRA after displacement does not influence the FRET measurement because upon displacement the molecules are too far from each other. This new setting confirms the influence that the polarity has on the T1117 emission and more importantly the specificity of T1117 binding to CB_1.

In Figure 2 panel d the two setting of the assay are described together with the procedure to measure the specific binding of T1117 to CB_1. For the measurement of binding to endogenous CB_1 or to recombinant CB_1, specific binding correlates with the specific quenching (difference in T1117 emission before and after displacement by AM251). In the presence of a fluorescent version of CB_1, like CB_1-GFP, the specific binding correlates with the change in the FRET dependent T1117 fluorescent emission.

Affinity and kinetic parameters of T1117 binding to CB_1 receptor. Binding of T1117 to CB_1 receptor was measured in a time course experiment at 1-min time intervals. After a short time (5 minutes) of equilibration of membranes in PBS, the indicated concentration of T1117 were added (Time 0, Fig. 3 a,b,c). As shown in Figure 3, an increase in fluorescence is visible till a plateau (less than 5% of fluorescence intensity variation per minute) is reached (association plateau, p_{ass}). Thus AM251 (Time 1, Fig. 3 a,b,c), was added to displace T1117 specifically bound to CB_1. As already seen with the measurement at equilibrium (Fig. 2a), the add of AM251 determines an increase of T1117 fluorescence till a second plateau is reached (dissociation plateau, p_{diss}). A similar increase was observed when 1 μM anandamide was added instead of AM251 at Time 1 (data not shown). Non cannabinoid receptors ligands such as nicotine (1 μM) did not affect the fluorescence of the probe (see Supplementary Figure S4).

The difference in fluorescence intensity between the two plateaus (ΔF) represents the amount of fluorescence that can be specifically dequenched by an excess of cannabinoid receptor ligands and thus is refereed as specific quenching.

Specific quenching correlates with the specific binding of T1117 and can be used to determine the affinity of the probe for cannabinoid receptors. When specific quenching is plotted *vs.* probe concentration, apparent B_{max} and K_d for T1117 can be calculated (Fig. 3d equation 1 in Appendix). As shown in Figure 3e, fluorescence signal correlates with T1117 concentration showing a correlation coefficient in untreated and AM251 treated membranes of 20248 $nM^{-1}cm^{-1}$ and 40427 $nM^{-1}cm^{-1}$, respectively. Using this titration curve, a value of 460 ± 80 nM and 10 ± 3 fmol/μg were calculated for K_d and B_{max} of the probe, respectively (Table 1). The specific quenching of T1117 was linear with protein concentration with optimal reproducible value obtainable using protein amount between 15 and 30 μg of total protein (Fig. 3 f).

The half time needed to displace T1117 by CB_1 directly correlates to k_{off} rate (see equation 2 in Appendix). k_{off} rate of displacement resulting from our measurement is 0.78 ± 0.2 min^{-1}. k_{obs} that directly correlates to the half time of association of T1117 and together with the measured k_{off} can be used to calculate k_{on} and K_d (equation 3–5 in Appendix). k_{on} and K_d measured with dynamic measurement were 1.76 ± 0.5 μM^{-1} min^{-1} and 431 ± 20 nM (Table 1).

T1117 as new tool to determine IC50 for orthosteric and allosteric Cannabinoid Receptor modulators. T1117 fluorescence measurement was tested as alternative tool to measure IC50 of ligands for Cannabinoid Receptors. Membranes were preincubated with different concentrations of the CB receptor agonist anandamide and the inverse agonist AM251 prior to addition of T1117 and the quenching of the probe was monitored in time (Fig. 4a–c). The treatment with increasing concentration of ligands resulted in an increase in the $p_{ass,}$ (Fig. 4a) as expected. Plotting the ratio between the fluorescent p_{ass} value of treated and untreated membranes (relative p_{ass}) versus concentration of the drug tested results in a conventional competition curve (Fig. 4b and c). IC50 values calculated for anandamide and AM251 are 21.0 ± 1.0 and 1.5 ±0.6 nM respectively, which are in accordance with those obtained using the radioligand displacement assay and reported in literature (IC50 anandamide = 40 nM[34];IC50 AM251 = 8 nM[32]).

Moreover we tested a further pool of 18 compounds for their ability to compete with T1117 in binding to CB_1 (see Supplementary Figure S4). Among the molecules we choose there are: i) hit molecules that came out from high throughput screening toward CB_1 receptor and displaying either high affinity and low affinity for the receptor[2] (compounds **4–6**); ii) molecules with features resembling the pharmacophore of an orthosteric ligand of CB_1[9,10], (compounds **7–11**); iii) a low affinity endogenous ligand for CB_1[2] (Oleamide); ligands of iv) COX enzymes (compound **12,** and Nimesulide); v) Nicotinic receptor (Nicotine, Epibatidine, Anabaseine); vi) 5HT3 receptor (Serotonine) and vii) GABA receptor (GABA). Rat brain membranes were incubated with T1117 for 30 minutes and then the compounds were added at the concentration of 1 μM. As shown in Supplementary figure S4 only the molecules belonging to

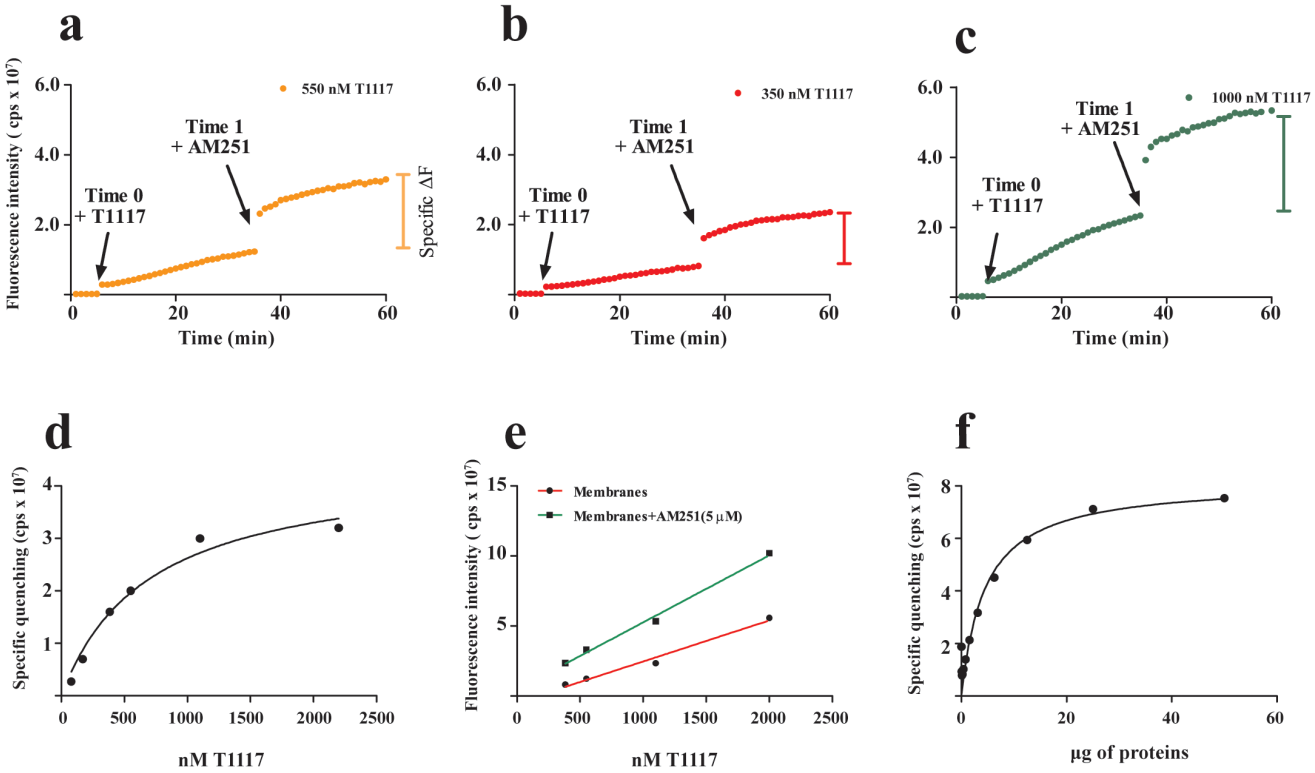

Figure 3 | Time-based scan of T1117 fluorescence. (a–c) Fluorescence at 610 nm was recorded at 1-min time intervals. After having been equilibrated in PBS, Rat brain membranes (15 μg of protein) were incubated at Time 0 with 350 nM (panel b) 550 nM (panel (a)) and 1000 nM (panel (c)) of T1117. After having reached a fluorescent plateau (p_{ass}) AM251 5 μM was added to the samples and fluorescence recorded till a second plateau (p_{diss}) was reached. Specific quenching (ΔF) (value of the fluorescence at p_{diss} minus the one at p_{ass}) is indicated. (d) Saturation isotherm constructed plotting specific quenching values versus T1117 concentration and fitting them with the equation 1 shown in the *Appendix*. (e) Rat brain membranes were incubated in the presence (squares) or in the absence (circles) of AM251 to be then incubated with the indicated concentration of T1117. Correlation between fluorescence intensity an amount of probe is represented using the linear regressions. (f) The indicated amount of membranes were incubated with 1000 nM T1117 to be then displaced with AM251 5 μM. Specific quenching was measured and plotted versus the amount of membranes used.

classes i, ii and iii were are able to displace T1117 at the tested concentration, confirming the specificity and sensitivity of the assay and its potentiality for high throughput screening toward CB_1. Interestingly, the assay also proved to be sensitive to small structural differences, being able to discriminate structurally related compounds as highlighted by compound **12**, which is structurally similar to AM251 (Fig. 1 and Supplementary Figure S4), but that does not displace T1117.

Similarly, T1117 fluorescence measurement can be employed to determine IC50 of the allosteric ligands such as ORG27569. ORG27569 is thought to induce a conformational change in CB_1 receptor that in turn increase and reduce the B_{max} for CB_1 of the agonist CP55940 and the inverse agonist AM251, respectively[23,24]. Using T1117 fluorescence measurement we indeed could measure a decrease in the amount of probe specifically bound to CB_1 (increase in relative p_{ass}) with an IC50 value for ORG27569 of 3.02 ± 1.05 μM (Fig. 4d), a value in a range similar of those reported in literature (IC50 ORG27569 (AM251) around 1 μM[16,19]). Since ORG27569 is an allosteric ligand specific for CB_1 receptor[16], our result show that T1117 is addressing mainly CB_1 receptor due to its specificity or to the low level of CB_2 and GPR55 in the rat brain membranes used.

Computational study ofAM251 and T1117 binding to CB_1. A three-dimensional model of CB_1 receptor was generated through the Modeller 9.11 software[35] (see Material and Methods for details) using as template the recently disclosed structure of human sphingosine 1-phosphate receptor [$S1P_1$ (PDB code: 3V2Y)][36]. The choice was dictated by the sequence identity and the close evolutionary relationship between the two receptors (see Supplementary Figures S5–S6 and Supporting Information for further details)[37]. For docking purpose, a box encompassing the entire orthosteric binding pocket as defined by mutagenesis data on Rimonabant (Fig. 1)[38–40] was applied. When AM251 was docked, the binding mode shown in Figure 5a was found (see Material and Methods for binding mode selection criteria). Specifically, the oxygen atom of the acetohydrazil group H-bonds to the $K^{3.28}$ amino group, the piperidinyl moiety is accommodate in a hydrophobic pocket defined by $F^{3.25}$, $K^{3.28}$, and $L^{3.29}$, while the 2,4-dichlorophenyl group establishes hydrophobic interaction with $F^{3.36}$, $W^{5.43}$, $W^{6.48}$, and $F^{2.61}$ residues and the *p*-iodophenyl group stacks between $F^{2.61}$ and $F^{7.35}$. The above-described biding mode (Fig. 5a) is in line with mutagenesis data indicating that the $F^{2.61}$, $K^{3.28}$, $L^{3.29}$, $F^{3.36}$, $W^{5.43}$, $W^{6.48}$, and $F^{7.35}$ residues are involved in Rimonabant binding[38–40], and it is in accordance with

Table 1 | T1117 Binding Parameters

	Kd	*Kon*	*Koff*	*Bmax*
Equilibium Binding	460 ± 80 nM			10 ± 3 fmol/μg
Dinamic Binding	431 ± 20 nM	1.76 ± 0.5 $\mu M^{-1}min^{-1}$	0.78 ± 0.2 min^{-1}	

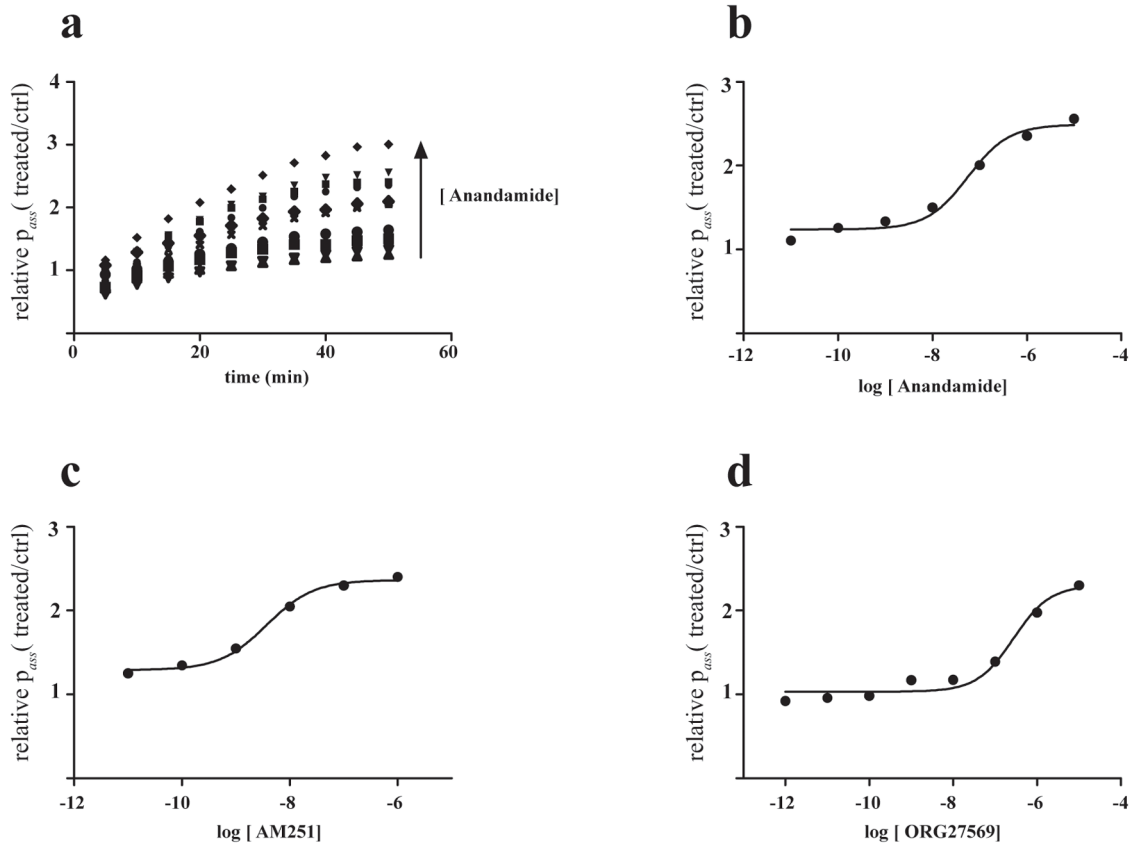

Figure 4 | T1117 fluorescence-quenching for affinity measurement of CB_1 ligands. Rat brain membranes were pre-incubated with increasing concentration of anandamide (panel (a–b)) AM251 (panel (c)) and ORG27569 (panel (d)), (the arrow indicate the increment in p_{ass} as the anandamide concentration increases). Fluorescence emission was recorded at the indicated time intervals after the add of T1117 and till a plateau was reached. Fluorescence fold difference at plateau (relative p_{ass}) is plotted versus anandamide (panel (b)) AM251 (panel (c)) and ORG27569 (panel (d)) concentration. Non linear regression (see equation 6 of Appendix) was used to fit the experimental values and calculate IC50 values.

SAR reported for this class of compounds[41,42]. In particular, SAR demonstrates that (*i*) the carbonyl moiety of the acetohydrazil group is essential for binding, in fact in our model it interacts with $K^{3.28}$; (*ii*) the elongation of the aliphatic chain at position 3 of the pyrazole ring leads to a reduction of the binding affinity, indeed in our model the piperidinyl substituent fills the above-described hydrophobic pocket; and (*iii*) bulky and hydrophobic substituents at position 5 of the pyrazole ring produced compounds with greater binding affinity for the CB_1 receptor[41,42]. In line with the proposed model, substituents at position 5 would extend toward the hydrophobic channel described below (see TAMRA positioning). Recently, a binding mode of Rimonabant which is rotated of 90° with respect to ours, facing the 5 position of the pyrazole ring towards the TM 5, was reported[40]. Such a difference is likely due to the different template used to build the CB_1 model (human β_2-adrenergic)[40]. However, the reported model would not explain the capability of T1117 to bind the CB_1 nor the tolerance of bulky substituents at position 5 of Rimonabant pyrazole ring[41,42]. Conversely, our docking of T1117 shows a binding mode similar to that observed for AM251 (Fig. 5b) in line with the experimentally found nanomolar K_d. However, the presence of the TAMRA group induces a slight shift of the entire compound, with respect to AM251, towards TM1 and TM7 (Fig. 5c) with the following consequences: (*i*) a weaker interaction with $K^{3.28}$ with respect to AM251, and (*ii*) worst interaction between the piperidinyl ring and $L^{3.29}$ with respect to AM251 (see Fig. 5a–c). Indeed, the phenylpropyl arm of TAMRA plunges in a hydrophobic channel defined by $I^{1.37}$, $F^{2.64}$, $A^{7.36}$, $F^{7.37}$, and $M^{7.40}$ while the rhodamine nucleus extends out of CB_1 soaking in the lipid environment (Fig. 5d). Taken together the binding modes found for AM251 and T1117 fully explain the nanomolar K_d of both compounds and clearly suggest that the "shifted" binding mode of T1117 is responsible for the reduced affinity of the latter with respect to AM251. The proposed binding mode for T1117 (Fig. 5b–d) is also able to explain the surprising fluorescence quenching of the probe upon binding to CB_1 (Fig. 2c). In our model, the TAMRA moiety appears in proximity of the polar heads of the phospholipids and of the TM7 domain of the protein (Fig. 5c, d). Thus, upon binding to CB_1, the fluorophore could be experiencing a more polar environment than in its unbound form. This model in turn provides a structural rationale to the quenching observed for T1117.

Discussion

Among conventional methods, radioligand displacement assay remains the most often used one for the discovery of new ligands for GPCRs. However, the need of high-throughput screening and high content drug discovery assay, together with the health, safety and disposal issues associated with the use of radioligands, has prompted a growing development of fluorescent based techniques.

Here, we report a detailed setting of the first fluorescent based assay in the Cannabinoid field. It makes use of a recently commercialized fluorescent analogue of the CB receptor inverse agonist AM251, namely T1117, derivatized with a tetra-methyl-rhodamine (TAMRA) moiety (Fig. 1).

T1117 shows a K_d for CB_1 receptor of around 450 nM, showing a lower affinity for the receptor than its non-fluorescent parental molecule (Fig. 1 and Table 1). The reduction in affinity compared to AM251 was expected and already seen for other fluorescent probe

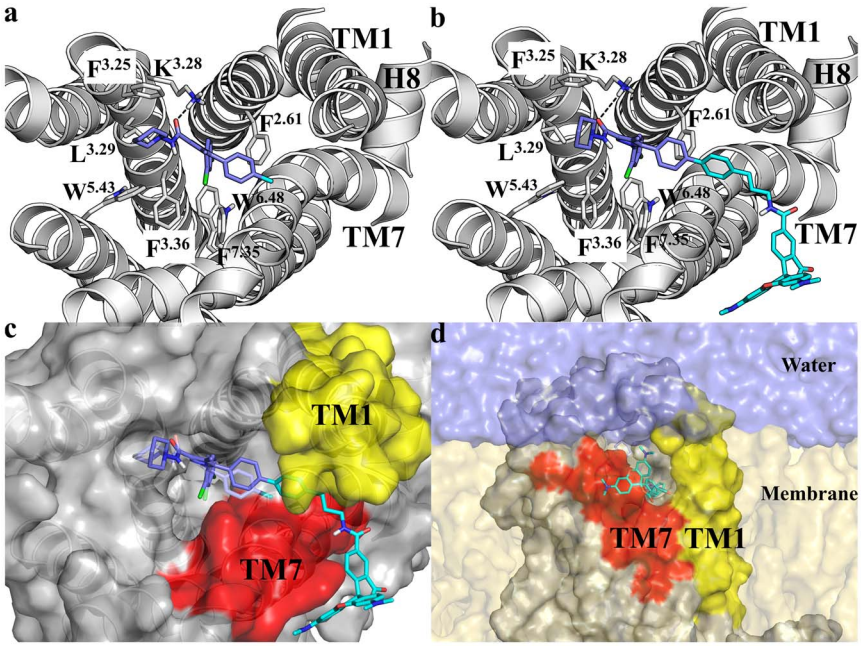

Figure 5 | Theoretical Binding modes of AM251 and T1117 within CB_1 receptor. (a) and (b) Binding poses of AM251 and T1117 respectively. The protein sidechains were represented in white sticks, the AM251 was depicted in light blue sticks, while the AM251 and TAMRA portion of T1117 were represented in light blue and cyan, respectively (c) Superposition of the AM251 and T1117 binding modes, the protein is represented by transparent, gray surface. TM7 and TM1 are highlighted by red and yellow surfaces, respectively. AM251 is represented by light blue and transparent sticks, while T1117 is depicted as indicated in (b). (d) Theoretical representation of the T1117 localization into the membrane environment. From the picture it can be appreciated how the TAMRA arm crosses the portal defined by TM1 and TM7 (yellow and red surface respectively).

bound to GPCR ligands[28,29]. Rodamine is a big molecule and it likely sterically hinders ligand-receptor interaction (Fig. 5).

The binding of T1117 to CB_1 is a two steps process. Driven by its poor solubility in water T1117 first moves into the lipid bilayer. The non polar environment of the membrane and the absence of quenching water molecules increases its fluorescence emission. Subsequently, T117 binds to CB_1 and gets fluorescently-quenched (Fig. 2 panel d).

The tendency to partition into membranes makes T1117 not ideal for *in situ* identification of CB_1 receptors (for example for staining of CB receptors in *in vitro* cultured cells) nor for being used as ligand for signaling studies (for example for functional assays on CB receptors). Under a fluorescence microscope it would be indeed not trivial to discriminate between specifically CB_1 bound T1117 from the one just absorbed into membranes. Similarly it would be difficult to attribute solely to a CB_1 modulation by T1117 the activation of a given intracellular pathway.

On contrary, T1117 expresses a great usefulness as displaceable ligand to measure affinity of agonists and inverse agonists of CB_1 receptors (Supplementary Figure S4). Affinities for anandamide and AM251 that were measured using our T1117 based assay are in perfect line with the ones obtained using other techniques reported in literature (Fig. 4). The fluorescence we follow has several advantages over conventional radioligand binding techniques including the ability to easily monitor ligand-receptor interactions in real time and determine kinetic parameters like k_{on} and k_{off} of binding (Fig. 3 and Table 1).

Using new generation fluorescence plate reader (see methods for detail) we have been able to perform binding measurement in a multiwell format and automatically dispense T1117 and the other components of the assay into the well increasing the accuracy for the measurement of kinetic parameters. This make our T1117 based assay an easy platform for the measurement of affinity of CB receptors orthosteric and allosteric ligands.

Although great strides have been done in the knowledge CB receptors, substantial challenges in understanding the mechanisms of orthosteric and allosteric ligands action at these receptors remain to be faced. Nowadays, allosteric ligands provide novel opportunities to modulate GPCR function that cannot be achieved by orthosteric ligands, however, much remain to be clarified about their functioning of allosteric ligands[18]. Herein, we prove that T1117 is sensitive to the allosteric drug ORG27569 and this would open up new precious opportunities for a better characterization of the allostery in CB receptors.

Besides reducing the considerable costs of a radio displacement assay, the T1117 based fluorescence experimental platform we describe has low environmental impact that together to its amenability for high-throughput screening and automation will prompt new contributions to the structural biology and the drug discovery in the CB receptors field.

Methods

Reagents. T1117 (Tocrifluor) (*N*-(Piperidin-1-yl)-5-(4-(4-(3-(5-carboxamido-tetramethylrhodaminyl)-propyl))phenyl)-1-(2,4-dichlorophenyl)-4-methyl-1*H*-pyrazole-3-carboxamide), AM251 (*N*-(Piperidin-1-yl)-5-(4-iodophenyl)-1-(2,4-dichlorophenyl)-4-methyl-1*H*-pyrazole-3-carboxamide) were from TOCRIS Bioscience. T1117 and AM251 were reconstituted in EtOH and diluted in PBS to 0.010 mM and 1,08 mM, respectively. Anandamide (*N*-(2-Hydroxyethyl)-5*Z*,8*Z*,11*Z*,14*Z*-eicosatetraenamide)was from Sigma Aldrich and was diluted to 1 mM. OR27569 (5-Chloro-3-ethyl-*N*-[2-[4-(1-piperidinyl)phenyl]ethyl-1*H*-indole-2-carboxamide) was kindly provided from R. Silvestri (University of Rome) and reconstituted 10 mM in DMSO. PBS tablets were from Fluka. Organic solvents from Carlo Erba (Italia). Compounds: **4** (2-(2-Chlorophenyl)-3-(4-chlorophenyl)-7-(2,2-difluoropropyl)-6,7-dihydro-2H-pyrazolo[3,4-f][1,4]oxazepin-8(5H)-one), **5** (5-(1,1-Dimethylheptyl)-2-[5-hydroxy-2-(3-hydroxypropyl)cyclohexyl]phenol), **6** (N-(4-chlorophenyl)-5-(4-(pentyloxy)phenyl)-1H-pyrazole-3-carboxamide), **7** (2-phenyl-2-norborbanol, mixture of endo and hexo), **8** (4-(2,5-diphenyl-2H-pyrazol-3-yl)-pyridine), **9** (1,5-Diphenyl-1H-pyrazole-4-carboxylic acid), **10** ((3-(4-isopropylphenyl)cyclohexyl)acetic acid, **11** (2-cyclohexylbenzoic acid), **12** (4-[5-(4-Methylphenyl)-3-(trifluoromethyl)-1H-pyrazol-1-yl]benzenesulfonamide), **13** (1,1′-(1,4-phenylene)bis(1-methylcyclohexane)), were purchased from Sigma-Aldrich Co.

LLC, Nicotine, Epibatidine, Serotonin, GABA, Anabasein, Oleamide, Quercetin, Nimesulide were all from Sigma Aldrich.

HEK 293 Culture, transfection and membrane preparation. HEK293-T were grown in DMEM supplemented with 5 mM Glutammine and 10% Fetal Calf Serum at 37° C in 5% CO_2 atmosphere. Freshly defrost cells were used for the transfection experiments. After a maximum of 7 days in culture cell were splitted the day before the experiment to gain a plate at 20–30% confluence. Poliethylenimmine (PEI) in water (1 μg/μl) was used as transfecting agent. Briefly 4 μg of DNA were mixed with 10 μg of PEI in 150 mM NaCl to be then added after 30 minutes of incubation to a 10 cm dish of cells in complete fresh medium. Cells were harvested 48 hours after the transfection and centrifuged for 5 minutes at 800× g, resuspended in cold PBS, and repelleted again. Cell pellet were dounced 20 times in a Teflon dounce. Homogenates were centrifuged for 5 minutes at 1,000× g (4°C) to remove nuclei, cell debris and unbroken cells. The resulting was centrifuged at 20,000× g to obtain a membrane fraction used for the fluorescence experiments.

Rat brain membranes preparation. Adult (300–400 g), male Sprague-Dawleyrats (kindly provided by Prof. Sorrentino and Prof. Ialenti, Faculty of Pharmacy, Naples, Italy) were killed by decapitation. The brains were rapidly removed and chilled in ice-cold PBS. Each organ was disrupted in 20 ml of cold PBS using a Teflon dounce (20 passages). The homogenates were centrifuged at 1,000× g (4°C) for 30 minutes to remove cell debris and unbroken tissues. The supernatant was centrifuged at 20,000× g to and the resulting pellet frozen on solid CO_2.

T1117 fluorescent measurement. 50 μl of membrane suspension (15 to 30 μg/μl of total proteins) in PBS were incubated in 96 well black Optiplate (Perkin Elmer) with or without the indicated amount of drugs. 5 minutes after the incubation the plates were inserted in a 2104 Envision Multi-label plate reader (Perkin Elmer). Each sample was excited with Envision filter 206 (535 ± 25 nM; 50% T) (Perkin Elmer) and fluorescence filtered with an emission filter 203 (615 ± 8.5 nM; 80% T) (Perkin Elmer), using a normal top mirror. Measurements were done in a continuous mode with time intervals of 1 minute. After 5 and 35 minutes the indicated amount of T1117 and AM251 dissolved in PBS were added to each well, respectively. The adding was performed using the automatic liquid dispenser of the Envision to dilute the two molecules at the indicated concentrations. Plots were fitted in Prism5 (**GraphPad Software Inc.**, La Jolla, CA) using inhibition sigmoidal curve to calculate IC50.

FACS measurement of T1117 binding to CB_1. HEK293 were transiently transfected with cDNA encoding for rat CB_1-GFP. 48 hours after the transfection cell were harvested by gentle resuspension in warm culture medium. While in suspension cells were treated with 1 μM T1117 for 30 minutes. When indicated, cells were treated for 15 minutes with 5 μM AM251. After being treated cells were sorted in a Bekton-Dickinson FACS-Sorted FACScan equipped with an Argon lamp in a linear data mode.

Absorbance measurement of T1117 binding to CB_1 and T117 partition into membranes. Rat brain membranes (60 μg) were incubated with the indicated amount T117 in a final volume of 100 μl for 15 minutes. When indicated 5 μM AM251 was added. Membranes were sedimented at 14.000 r.p.m. in a tabletop centrifuge at 4°C. Pellets were resuspended in PBS and absorbance measured at 530 nm and plotted versus T1117 concentration. Data were fitted with equation 1 of the Appendix section in Graph Pad Prism.

Fluorescence scan of T1117 binding to CB_1. Rat brain membranes (150 μg) were incubated with 500 nM T117 for 15 minutes in a quartz cuvette in the dark in a finale volume of 500 μl. Fluorescence spectra were recorded in a Cary Eclipse Spectrophofomoter at R.T. with $\lambda_{exc} = 530$ nm and λ_{ems} in the 550 to 700 nm range. Excitation and emission slits were set at 5 nm.

FRET measurement of T1117 binding to CB_1-GFP. HEK293 cells transiently expressing CB_1-GFP were harvested and processed as described above. Samples were excited with Envision filter 102 (485 ± 14 nM; 60% T) (Perkin Elmer) and fluorescence filtered with an emission filter 203 (615 ± 8.5 nM; 80% T) (Perkin Elmer), with a time delay between excitation and emission of 90 ms.

Homology modelling. To date, a number of X-ray crystal structures for different GPCR families were disclosed[43,44]. In this context, several models of the CB_1 receptor have been proposed using rhodopsin, β_2-adrenergic and adenosine receptor subtype 2A (A_{2A})as template[40,45,46]. Among the possible CB_1 templates, recently, the human sphingosine 1-phosphate receptor ($S1P_1$) has been disclosed offering new possibility to build up more reliable 3D model for the CB_1 receptor[37]. In fact, receptors having the highest sequence identity with respect to the CB_1 are the $S1P_1$ and the A_{2A}{27% and 23% of sequence identity, respectively [(data obtained from the ClustalW identity matrix)[47] see Supplementary Figure S5]}. Moreover, $S1P_1$ orthosteric binding site was evolutionary selected to bind sphingosine (a lipid-derived ligand) and similarly CB_1 binds a lipid-derived ligand (anandamide) as transmitter[9]. In addition, experimental evidences support the notion that CB_1 and $S1P_1$ share a common mechanism of binding and a common activation mechanism[37]. Therefore, the $S1P_1$ X-ray crystal structure (pdb code: 3V2Y[36]) was choose and used as template to generate the 3D structure of CB_1. CB_1 and $S1P_1$sequences were aligned using the ClustalW server[47] (see Supplementary Figure S6) and the 3D model of CB_1 was generated using the Modeller9.11 software[35].

Molecular docking. AM251and T1117 were built using the fragment builder tool of Maestro9.1[48]. The compounds were geometrically optimized by means of Macromodel[48], using MMFFs as force field, water as implicit solvent until a convergence value of 0.05 kcal/mol*Å^2. The computational protocol applied consists of the application of 500 steps of the Polak-Ribiére conjugate gradient (PRCG) for structure minimizations. The CB_1 protein structure was prepared through the Protein Preparation Wizard of Maestro9.1[48]. Docking was accomplished through the Glide induced fit docking (IFD) tool available in Maestro9.1[48]. The grid was centered on the residues shaping the orthosteric binding pocket for which mutagenesis data on Rimonabant binding are available[38–40] ($F^{2.61}$, $K^{3.28}$, $L^{3.29}$, $F^{3.36}$, $W^{5.43}$, $W^{6.48}$, and $F^{7.35}$ according to Ballesteros−Weinstein numbering[49]). The flexible region of the protein was fixed until 8 Å around the center of the grid. Each docking run was carried out with the standard precision (SP) method, and the van deer Waals scaling factor of non polar atoms was set to 0.8. Fifteen docking poses were obtained and among these poses we selected the best pose in accordance with the mutagenesis data[38–40], and structure-activity relationship studies previously reported for this class of CB_1 ligands[41,42]. Finally, T1117 was docked using as reference structure the selected CB_1-AM251 complex. Since the large dimension of the TAMRA substituent of T1117 the Glide induced fit docking (IFD) tool available in Maestro9.1 was used[48]. In this case the grid for the docking studies was centered directly on the AM251 ligand binding pose. The flexible region was fixed until 8 Å around the center of the grid. Each docking run was carried out with the standard precision (SP) method, and the van deer Waals scaling factor of non polar atoms was set to 0.8. Fifteen docking poses were obtained and among these poses we selected the docking pose with the highest Glide score. The selected docking pose were minimized using OPLSA2005 as force field, the PRCG methods until a gradient of 0.001 kcal/mol*Å^2 applying a stepwise relaxation protocol for which harmonic constraints were progressively reduced for backbone, side chains and ligand atoms.

CB_1cDNA. Homo sapiens CB_1 receptor cDNA (CNR1, NM_016083) already cloned in the vector pCMV6-XL4 was purchased at Origene Technologies. The DNA was amplified and maxi-prep (Quiagen) pure DNA was used for transfection. The construct encoding the rat CB_1, C-terminally tagged with GFP (3xFLAG- CB_1Rwt-GFP) was kindly provided by Prof. Zsolt Lenkei (ESPCI Paris)[50].

1. Pacher, P. & Kunos, G. Modulating the endocannabinoid system in human health and disease - successes and failures. *Febs J.* **280**, 1918–1943 (2013).
2. Pertwee, R. G. Targeting the endocannabinoid system with cannabinoid receptor agonists: pharmacological strategies and therapeutic possibilities. *Philos. Trans. R. Soc. B Biol. Sci.* **367**, 3353–3363 (2012).
3. di Marzo, V. D., Bifulco, M. & Petrocellis, L. D. The endocannabinoid system and its therapeutic exploitation. *Nat. Rev. Drug Discov.* **3**, 771–784 (2004).
4. Matsuda, L. A., Lolait, S. J., Brownstein, M. J., Young, A. C. & Bonner, T. I. Structure of a cannabinoid receptor and functional expression of the cloned cDNA. *Nature* **346**, 561–564 (1990).
5. Munro, S., Thomas, K. L. & Abu-Shaar, M. Molecular characterization of a peripheral receptor for cannabinoids. *Nature* **365**, 61–65 (1993).
6. Ryberg, E. *et al.* The orphan receptor GPR55 is a novel cannabinoid receptor. *Br. J. Pharmacol.* **152**, 1092–1101 (2007).
7. Piomelli, D. The molecular logic of endocannabinoid signalling. *Nat. Rev. Neurosci.* **4**, 873–884 (2003).
8. Freund, T. F., Katona, I. & Piomelli, D. Role of endogenous cannabinoids in synaptic signaling. *Physiol. Rev.* **83**, 1017–1066 (2003).
9. Castillo, P. E., Younts, T. J., Chávez, A. E. & Hashimotodani, Y. Endocannabinoid Signaling and Synaptic Function. *Neuron* **76**, 70–81 (2012).
10. Petrocellis, L. D., Cascio, M. G. & Marzo, V. D. The endocannabinoid system: a general view and latest additions. *Br. J. Pharmacol.* **141**, 765–774 (2004).
11. Pertwee, R. G. Inverse agonism and neutral antagonism at cannabinoid CB_1 receptors. *Life Sci.* **76**, 1307–1324 (2005).
12. Frank, B., Serpell, M. G., Hughes, J., Matthews, J. N. S. & Kapur, D. Comparison of analgesic effects and patient tolerability of nabilone and dihydrocodeine for chronic neuropathic pain: randomised, crossover, double blind study. *BMJ* **336**, 199–201 (2008).
13. Pertwee, R. G. The pharmacology of cannabinoid receptors and their ligands: an overview. *Int. J. Obes. 2005* **30 Suppl 1**, S13–18 (2006).
14. Blake, D. R. Preliminary assessment of the efficacy, tolerability and safety of a cannabis-based medicine (Sativex) in the treatment of pain caused by rheumatoid arthritis. *Rheumatology* **45**, 50–52 (2006).
15. Rosengren, R. & Cridge, B. Critical appraisal of the potential use of cannabinoids in cancer management. *Cancer Manag. Res.* **5**, 301–313 (2013).
16. Price, M. R. *et al.* Allosteric modulation of the cannabinoid CB_1 receptor. *Mol. Pharmacol.* **68**, 1484–1495 (2005).
17. Piscitelli, F. *et al.* Indole-2-carboxamides as Allosteric Modulators of the Cannabinoid CB_1 Receptor. *J. Med. Chem.* **55**, 5627–5631 (2012).
18. Wootten, D., Christopoulos, A. & Sexton, P. M. Emerging paradigms in GPCR allostery: implications for drug discovery. *Nat. Rev. Drug Discov.* **12**, 630–644 (2013).

19. Ross, R. A. Allosterism and cannabinoid CB(1) receptors: the shape of things to come. *Trends Pharmacol. Sci.* **28**, 567–572 (2007).
20. Cawston, E. E. *et al.* Real-time characterisation of Cannabinoid Receptor 1 (CB_1) allosteric modulators reveals novel mechanism of action.: Allosteric Modulators of CB_1. *Br. J. Pharmacol.* **170**, 893–907 (2013).
21. Ahn, K. H., Mahmoud, M. M. & Kendall, D. A. Allosteric Modulator ORG27569 Induces CB_1 Cannabinoid Receptor High Affinity Agonist Binding State, Receptor Internalization, and Gi Protein-independent ERK1/2 Kinase Activation. *J. Biol. Chem.* **287**, 12070–12082 (2012).
22. Ahn, K. H., Mahmoud, M. M., Shim, J.-Y. & Kendall, D. A. Distinct Roles of b-Arrestin 1 and b-Arrestin 2 in ORG27569-induced Biased Signaling and Internalization of the Cannabinoid Receptor 1 (CB_1). *J. Biol. Chem.* **288**, 9790–9800 (2013).
23. Fay, J. F. & Farrens, D. L. A key agonist-induced conformational change in the cannabinoid receptor CB_1 is blocked by the allosteric ligand Org 27569. *J. Biol. Chem.* **287**, 33873–33882 (2012).
24. Baillie, G. L. *et al.* CB_1 Receptor Allosteric Modulators Display Both Agonist and Signaling Pathway Specificity. *Mol. Pharmacol.* **83**, 322–338 (2012).
25. Devane, W. A., Dysarz, F. A. 3rd., Johnson, M. R., Melvin, L. S. & Howlett, A. C. Determination and characterization of a cannabinoid receptor in rat brain. *Mol. Pharmacol.* **34**, 605–613 (1988).
26. Roth, S. H. & Williams, P. J. The non-specific membrane binding properties of delta9-tetrahydrocannabinol and the effects of various solubilizers. *J. Pharm. Pharmacol.* **31**, 224–230 (1979).
27. Harris, L. S., Carchman, R. A. & Martin, B. R. Evidence for the existence of specific cannabinoid binding sites. *Life Sci.* **22**, 1131–1137 (1978).
28. Middleton, R. J. & Kellam, B. Fluorophore-tagged GPCR ligands. *Curr. Opin. Chem. Biol.* **9**, 517–525 (2005).
29. Martín-Couce, L. *et al.* Chemical Probes for the Recognition of Cannabinoid Receptors in Native Systems. *Angew. Chem. Int. Ed.* **51**, 6896–6899 (2012).
30. Daly, C. J. *et al.* Fluorescent ligand binding reveals heterogeneous distribution of adrenoceptors and 'cannabinoid-like' receptors in small arteries. *Br. J. Pharmacol.* **159**, 787–796 (2010).
31. Sylantyev, S., Jensen, T. P., Ross, R. A. & Rusakov, D. A. Cannabinoid- and lysophosphatidylinositol-sensitive receptor GPR55 boosts neurotransmitter release at central synapses. *Proc. Natl. Acad. Sci. U. S. A.* **110**, 5193–5198 (2013).
32. Gatley, S. J. *et al.* Binding of the non-classical cannabinoid CP 55,940, and the diarylpyrazole AM251 to rodent brain cannabinoid receptors. *Life Sci.* **61**, PL 191–197 (1997).
33. Havunjian, R. H., De Costa, B. R., Rice, K. C. & Skolnick, P. Characterization of benzodiazepine receptors with a fluorescence-quenching ligand. *J. Biol. Chem.* **265**, 22181–22186 (1990).
34. Devane, W. A. *et al.* Isolation and structure of a brain constituent that binds to the cannabinoid receptor. *Science* **258**, 1946–1949 (1992).
35. MODELLER, Program for Comparative Protein Structure Modelling by Satisfaction of Spatial Restraints, http://salilab.org/modeller.
36. Hanson, M. A. *et al.* Crystal Structure of a Lipid G Protein-Coupled Receptor. *Science* **335**, 851–855 (2012).
37. Hurst, D. P., Schmeisser, M. & Reggio, P. H. Endogenous lipid activated G protein-coupled receptors: Emerging structural features from crystallography and molecular dynamics simulations. *Chem. Phys. Lipids* **169**, 46–56 (2013).
38. Hurst, D. P. *et al.* N-(piperidin-1-yl)-5-(4-chlorophenyl)-1-(2,4-dichlorophenyl)-4-methyl-1H-pyrazole-3-carboxamide (SR141716A) interaction with LYS 3.28(192) is crucial for its inverse agonism at the cannabinoid CB_1 receptor. *Mol. Pharmacol.* **62**, 1274–1287 (2002).
39. McAllister, S. D. *et al.* An aromatic microdomain at the cannabinoid CB(1) receptor constitutes an agonist/inverse agonist binding region. *J. Med. Chem.* **46**, 5139–5152 (2003).
40. Shim, J.-Y., Bertalovitz, A. C. & Kendall, D. A. Probing the Interaction of SR141716A with the CB1 Receptor. *J. Biol. Chem.* **287**, 38741–38754 (2012).
41. Wiley, J. L. *et al.* Novel pyrazole cannabinoids: insights into CB(1) receptor recognition and activation. *J. Pharmacol. Exp. Ther.* **296**, 1013–1022 (2001).
42. Lan, R. *et al.* Structure-activity relationships of pyrazole derivatives as cannabinoid receptor antagonists. *J. Med. Chem.* **42**, 769–776 (1999).
43. Katritch, V., Cherezov, V. & Stevens, R. C. Structure-Function of the G Protein–Coupled Receptor Superfamily. *Annu. Rev. Pharmacol. Toxicol.* **53**, 531–556 (2013).
44. Venkatakrishnan, A. J. *et al.* Molecular signatures of G-protein-coupled receptors. *Nature* **494**, 185–194 (2013).
45. Salo, O. M. H., Lahtela-Kakkonen, M., Gynther, J., Järvinen, T. & Poso, A. Development of a 3D model for the human cannabinoid CB_1 receptor. *J. Med. Chem.* **47**, 3048–3057 (2004).
46. Oddi, S. *et al.* Effects of palmitoylation of Cys415 in helix 8 of the CB_1 cannabinoid receptor on membrane localization and signalling: CB_1 receptor palmitoylation. *Br. J. Pharmacol.* **165**, 2635–2651 (2012).
47. Lopez, R. ClustalWW – WWW Service at the European Bionformatics Institute, http://www.ebi.ac.uk/Tools/msa/clustalw2/, date of acces May 2013.
48. Schrödinger, Mestro version 9.1 Schrödinger, LLC, New York 2009.
49. Ballesteros, J. A. & Weinstein, H. Integrated methods for the construction of three-dimensional models and computational probing of structure-function relations in G protein-coupled receptors. *Methods Neurosci.* **25**, 366–428 (1995).
50. Leterrier, C., Bonnard, D., Carrel, D., Rossier, J. & Lenkei, Z. Constitutive endocytic cycle of the CB_1 Cannabinoid Receptor. *J. Biol. Chem.* **279**, 36013–36021 (2004).

Acknowledgments

We thank Prof. Zsolt Lenkei for providing us with the construct expressing Flag-CB_1RWT-EGFP. We thank Dr. Fiammetta Romano and Dr. Mario Masullo for the help provided during FACS analysis and spectra recording. We thank Sara Bottone for her technical support. We thank Alex Fish, Jens Hausmann and Vera Roberti for fruitful discussions.

Author contributions

The experimental work was performed by A.B. and M.S. A.B., F.L., E.N., M.S. and L.M. planned the work and analyzed the results. The paper was written by M.S., A.B. and L.M. with assistance from the other authors.

Additional information

Supplementary information accompanies this paper at http://www.nature.com/scientificreports

Competing financial interests: The authors declare no competing financial interests.

How to cite this article: Bruno, A., Lembo, F., Novellino, E., Stornaiuolo, M. & Marinelli, L. Beyond radio-displacement techniques for Identification of CB_1 Ligands: The First Application of a Fluorescence-quenching Assay. *Sci. Rep.* **4**, 3757; DOI:10.1038/srep03757 (2014).